数理解析研究所講究録
1493巻 2006年 153-165

Fast Diffusion in Multi-Degree-of-Freedom Hamiltonian Systems with Saddle-Centers

岐阜大学工学部　矢ヶ崎一幸 (Kazuyuki Yagasaki)
Faculty of Engineering, Gifu University

1. Introduction

We study $(n+1)$-degree-of-freedom Hamiltonian systems $(n \geq 2)$ of the form

$$\dot{x} = J_1 \mathrm{D}_x H(x,y), \quad \dot{y} = J_n \mathrm{D}_y H(x,y), \quad (x,y) \in \mathbb{R}^2 \times \mathbb{R}^{2n}, \tag{1}$$

where $H : \mathbb{R}^2 \times \mathbb{R}^{2n} \to \mathbb{R}$ is C^{r+1} $(r \geq 2n+4)$, and J_m is the $2m \times 2m$ symplectic matrix,

$$J_m = \begin{pmatrix} 0 & \mathrm{id}^m \\ -\mathrm{id}^m & 0 \end{pmatrix}$$

with id^m the $m \times m$ identity matrix. We especially assume that the x-plane is invariant under the flow of (1) and there is a saddle-center with n pairs of purely imaginary eigenvalues at the origin $(x,y) = (0,0)$ $(= O)$ having a homoclinic orbit on the x-plane (see Section 2 for our precise assumptions). In this situation, there exist n-dimensional whiskered invariant tori near the saddle-center.

We consider small perturbations near the homoclinic orbits, and develop a Melnikov-type technique for detecting the existence of orbits transversely homoclinic or heteroclinic to the invariant tori. Note that the system (1) does not take the form of a small perturbation of an integrable system unlike many other versions of Melnikov-type methods (e.g., [5, 10]). We also show that Arnold diffusion type motions occur if such heteroclinic orbits exist. Numerical evidence of fast diffusion for a specific three-degree-of-freedom system is given.

Similar methods are also applicable to two-degree-of-freedom Hamiltonian systems and (four-dimensional) reversible systems. We briefly describe the methods and the relation with the differential Galois theory for nonintegrability [8] in the two-degree-of-freedom Hamiltonian case. See [11–16] for backgrounds and details on these results.

2. Assumptions

We make the following assumptions on (1).

(A1) $\mathrm{D}_x H(0,0) = 0$ and $\mathrm{D}_y H(x,0) = 0$ for any $x \in \mathbb{R}^2$.

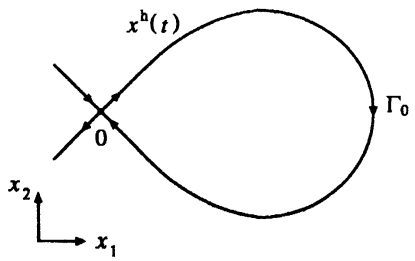

Fig. 1. The phase portrait on the x-plane.

Assumption (A1) means that the origin O is an equilibrium of (1) and the x-plane, $\{(x,y) \in \mathbb{R}^2 \times \mathbb{R}^{2n} \mid y = 0\}$, is invariant under the flow of (1). The system restricted on the x-plane,

$$\dot{x} = J_1 \mathrm{D}_x H(x,0), \tag{2}$$

has an equilibrium at $x = 0$. Moreover, $\mathrm{D}_x^j \mathrm{D}_y H(x,0) = 0$, $j = 1,2,\ldots$, for any $x \in \mathbb{R}^2$.

(A2) The equilibrium $x = 0$ of (2) is a hyperbolic saddle and has a homoclinic orbit $x^h(t)$. Let $\Gamma_0 = \{x = x^h(t) | t \in \mathbb{R}\} \cup \{0\}$. See Fig. 1.

(A3) The matrix $J_n \mathrm{D}_y^2 H(0,0)$ has n pairs of purely imaginary, nonzero eigenvalues $\pm \mathrm{i}\,\omega_j$, $j = 1,\ldots,n$. In addition, the nonresonance condition

$$k \cdot \omega = k_1\omega_1 + \cdots + k_n\omega_n \neq 0 \tag{3}$$

holds for any $k = (k_1,\ldots,k_n) \in \mathbb{Z}^n$ such that $1 \leq |k| = \sum_{j=1}^n k_j \leq 4$, where "$\cdot$" represents the inner product and $\omega = (\omega_1,\ldots,\omega_n)$.

Assumptions (A2) and (A3) mean that the equilibrium O is a saddle-center and has a homoclinic orbit $(x,y) = (x^h(t),0)$. It follows from the center manifold theory (e.g., [9]) that the saddle-center O has a C^r, $2n$-dimensional local center manifold, $W^c_{\mathrm{loc}}(O)$, which may be non-unique, as well as C^r, one-dimensional stable and unstable manifolds, $W^s(O)$ and $W^u(O)$, which coincide along the homoclinic orbit $(x^h(t),0)$. By assumption (A2), the two eigenvalues of $J_1 \mathrm{D}_x^2 H(0,0)$ is expressed as $\pm\lambda$, where λ is a positive real number (see Section II.C of [7]).

Under the above assumptions, using arguments given in the proof of Lemma 4 of [3] and noting H is at least C^5, we prove that there is a symplectic transformation $(x,y) \mapsto (s,u,I,\psi) \in \mathbb{R} \times \mathbb{R} \times \mathbb{R}^n \times \mathbb{T}^n$ such that the Hamiltonian H can be expressed as the following normal form

$$H(s,u,I,\psi) = \lambda su + \omega \cdot I + \frac{1}{2}(AI \cdot I) + g(s,u,I,\psi) \tag{4}$$

near the saddle-center O, where A is an $n \times n$ matrix, and $g : \mathbb{R} \times \mathbb{R} \times \mathbb{R}^n \times \mathbb{T}^n \to \mathbb{R}$ is C^{r+1} for $I \neq 0$ and of higher order than 2 in s, u and I. Here $\mathbb{T}^n = \prod_{j=1}^n \mathbb{S}^1$ is the n-torus

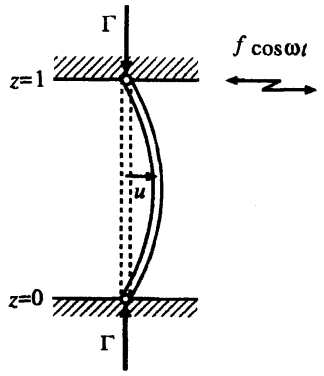

Fig. 2. Forced vibrations of a buckled beam.

with $\mathbb{S}^1$ the circle of length 2π. In the light of this observation, the following assumption is made.

(A4) The matrix A is nonsingular.

Under assumptions (A1)-(A4), on $W^c(O)$ near O there exists a Cantor set of n-dimensional invariant tori $\mathscr{T}_\nu$ consisting of quasiperiodic orbits with n frequencies ν_j close to ω_j, $j = 1, \ldots, n$, such that the Diophantine condition,

$$k \cdot \nu > c\,|k|^{-\tau} \quad \text{for } k \in \mathbb{Z}^n \text{ and } k \neq 0, \tag{5}$$

holds, where $\nu = (\nu_1, \ldots, \nu_n)$, and $c > 0$ and $\tau > n - 1$ are constants. The invariant torus $\mathscr{T}_\nu$ is whiskered, i.e., it has $(n+1)$-dimensional stable and unstable manifolds, $W^s(\mathscr{T}_\nu)$ and $W^u(\mathscr{T}_\nu)$.

Let

$$p(x, \eta) = \frac{1}{2} \mathrm{D}_y^2 f(x, 0)(\eta, \eta)$$

with $f(x, y) = J_1 \mathrm{D}_x H(x, y)$, where $\eta \in \mathbb{R}^{2n}$. Finally, we assume the following.

(A5) $p(x, \eta) \not\equiv 0$.

3. Motivated example: Free vibrations of an undamped, buckled beam

Holmes and Marsden [6] proved that chaotic motions exist in the partial-integral differential equation

$$\ddot{u} + u'''' + \left[\Gamma - \kappa \int_0^1 (u')^2 \mathrm{d}\zeta\right] u'' = \epsilon(f \cos \omega t - \delta \dot{u}) \tag{6}$$

under the boundary conditions

$$u(0) = u(1) = 0, \quad u''(0) = u''(1) = 0.$$

Eq.(6) represents a mathematical model for forced vibrations of a damped, buckled beam shown in Fig. 2. This is one of the earliest examples of infinite dimensional systems in which the existence of chaos was mathematically proven. Now we have the following question: What dynamics does the buckled beam exhibit without damping and external force?

To answer this question, we expand solutions of (6) as

$$u(z,t) = \sum_{l=1}^{n+1} a_l(t) \sin j_l \pi z, \quad j_1 = 1, \quad 1 < j_2 < \cdots < j_{n+1}, \quad n \geq 1. \tag{7}$$

Substituting (7) into (6) and changing the state variables as

$$(a_1, \dot{a}_1, a_{l+1}, \dot{a}_{l+1}) \mapsto (x_1, x_2, y_1, y_{l+n}),$$

we obtain a Hamiltonian system with the Hamiltonian

$$H_n(x,y) = \frac{1}{2}\left(-x_1^2 + \sum_{l=1}^{n} \omega_l^2 y_l^2\right) + \frac{1}{4}\left(x_1^2 + \sum_{l=1}^{n} j_{l+1}^2 y_l^2\right)^2 + \frac{1}{2}\left(x_2^2 + \sum_{l=1}^{n} y_{n+l}^2\right) \tag{8}$$

in the nondimensional form, where $\omega_l = j_{l+1}\sqrt{(j_{l+1}^2\pi^2 - \Gamma)/(\Gamma - \pi^2)}$. Note that any approximations are not required here. We easily see that all the assumptions of Section 2 are satisfied if $\pi^2 < \gamma < j_2^2\pi^2$ and the resonance condition (3) up to fourth-order holds for $1 \leq |k| \leq 4$. See [12] for more details. As we see in Section 5, our theory can answer the above question.

4. Main results

Consider variational equations of (1) in the y-direction about the saddle-center O and homoclinic orbit $(x,y) = (x^{\mathrm{h}}(t), 0)$,

$$\dot{\eta} = J_n \mathrm{D}_y^2 H(0,0)\eta \tag{9}$$

and

$$\dot{\eta} = J_n \mathrm{D}_y^2 H(x^{\mathrm{h}}(t), 0)\eta. \tag{10}$$

We call (10) the *normal variational equation* of (1) along $x^{\mathrm{h}}(t)$. We can express a fundamental matrix to (9) as $\Phi(\omega_1 t, \ldots, \omega_n t)$, where Φ is 2π-periodic in each arguments and $\Phi(0, \ldots, 0) = \mathrm{id}^{2n}$. Let $\Psi(t)$ be a fundamental matrix to (10). Using a standard result about asymptotic behavior of linear systems (e.g., Section 3.8 of [1]), we see that the limits

$$B_{\pm} = \lim_{t \to \pm\infty} \Phi(-\omega t)\, \Psi(t) \tag{11}$$

exist. Obviously, $B_{\pm}$ are nonsingular matrices and we set $B_0 = B_+ B_-^{-1}$.

Let e_j be a $2n$-dimensional real vector belonging to a two-dimensional linear vector space spanned by eigenvectors for eigenvalues $\pm \mathrm{i}\,\omega_j$ of $J_n \mathrm{D}_y^2 H(0,0)$, and let

$$\bar{\eta}_r = \sum_{j=1}^{n} r_j e_j \tag{12}$$

for $r = (r_1, \ldots, r_n) \in \mathbb{R}^n_+$, where $\mathbb{R}^n_+ = \prod_{j=1}^n (0, \infty)$. Denote

$$q(\eta) = \frac{1}{2} \mathrm{D}_y^2 H(0,0)(\eta, \eta)$$

for $\eta \in \mathbb{R}^{2n}$. We define the *Melnikov function* $M(\theta; r)$ as

$$M(\theta; r) = q(\bar{\eta}_r) - q(B_0 \Phi(\theta) \bar{\eta}_r). \tag{13}$$

The Melnikov function M depends not only on $\theta \in \mathbb{T}^n$ but also on $r \in \mathbb{R}^n_+$ while it was defined as a function of only a scalar variable when $n = 1$ (see Eq. (23). We prove the following theorem.

Theorem 1 (i) *Suppose that there is a point $(\theta, r) = (\theta_0, r_0) \in \mathbb{T}^n \times \mathbb{R}^n_+$ such that*

$$M(\theta_0; r_0) = 0 \quad \textit{and} \quad \frac{\partial}{\partial \theta_j} M(\theta_0; r_0) \neq 0, \quad j = 1, \ldots, n. \tag{14}$$

Then near the saddle-center O there exist whiskered invariant tori $\mathcal{T}_{\nu^1}$ and $\mathcal{T}_{\nu^2}$, respectively, consisting of quasiperiodic orbits with frequency vectors ν^1 and ν^2, such that on the energy surface of $\mathcal{T}_{\nu^1}$ and $\mathcal{T}_{\nu^2}$ $W^{\mathrm{u}}(\mathcal{T}_{\nu^1})$ intersects $W^{\mathrm{s}}(\mathcal{T}_{\nu^2})$ transversely, where ν^j, $j = 1, 2$, are close to ω and satisfy the Diophantine condition (5). If $\Phi(\tilde{\theta}_0)\bar{\eta}_{r_0} = B_0 \Phi(\theta_0)\bar{\eta}_{r_0}$ for some $\tilde{\theta}_0 \in \mathbb{T}^n$, one can set $\nu^1 = \nu^2$ in this statement, i.e., there exist orbits transversely homoclinic to $\mathcal{T}_\nu$, where $\nu = \nu^1 = \nu^2$.

(ii) *Suppose that there are $\theta^j \in \mathbb{T}^n$, $j = 1, \ldots, N-1$, and $r^j \in \mathbb{R}^n_+$, $j = 1, \ldots, N$, such that condition (14) holds for $(\theta_0, r_0) = (\theta^j, r^j)$, $j = 1, \ldots, N-1$, and $\Phi(\tilde{\theta}^j)\bar{\eta}_{r^{j+1}} = B_0 \Phi(\theta^j)\bar{\eta}_{r^j}$ for some $\tilde{\theta}^j \in \mathbb{T}^n$, $j = 1, \ldots, N-1$. Then near O there exist N whiskered invariant tori $\mathcal{T}_{\nu^j}$, $j = 1, \ldots, N$, consisting of quasiperiodic orbits with frequency vectors ν^j, $j = 1, \ldots, N$, close to ω and satisfying (5), such that on their energy surface $W^{\mathrm{u}}(\mathcal{T}_{\nu^j})$ intersects $W^{\mathrm{s}}(\mathcal{T}_{\nu^{j+1}})$ transversely.*

See [15] for the proof. A sequence of invariant tori such as $\mathcal{T}_{\nu^j}$, $j = 1, \ldots, N$, in Theorem 1 (ii) is called a *transition chain*.

Theorem 2 *Suppose that in the Hamiltonian system (1) there is a transition chain of N whiskered invariant tori $\mathcal{T}_j$, $j = 1, \ldots, N$, consisting of quasiperiodic orbits with irrational frequencies (see Fig. 3). Then there exists an open set of points arbitrarily close to $\mathcal{T}_1$ connected by trajectories with points arbitrarily close to $\mathcal{T}_N$ through points near $\mathcal{T}_j$, $j = 2, \ldots, N-1$, in turn.*

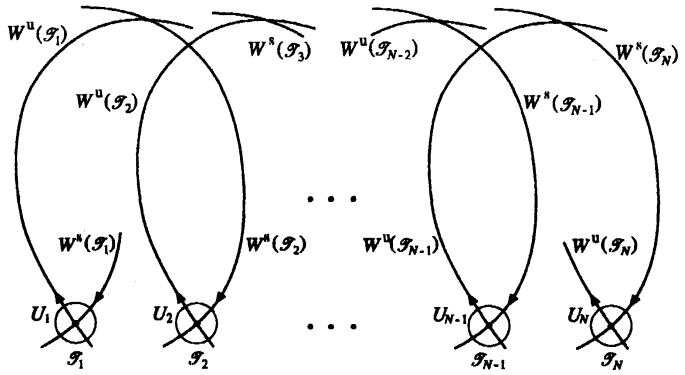

Fig. 3. Arnold diffusion type motions.

See [15] for the proof.

The behavior detected by Theorem 2 is similar to Arnold diffusion in near-integrable systems (see Section 1) although the drift speed can be very fast. In the situation of Theorem 1(ii) it is $\mathcal{O}(\epsilon)$. We call this behavior in not near-integrable systems *Arnold diffusion type* motions. For a transition chain of N whiskered invariant tori $\{\mathscr{T}_1, \ldots, \mathscr{T}_N\}$, one may have $\mathscr{T}_1 = \mathscr{T}_N$. We say that such a transition chain is *cyclic*.

Suppose that there are two distinct, cyclic transition chains of $N_1 + 2$ and $N_2 + 2$ whiskered invariant tori, $\{\mathscr{T}_0, \mathscr{T}_1^1, \ldots, \mathscr{T}_{N_1}^1, \mathscr{T}_0\}$ and $\{\mathscr{T}_0, \mathscr{T}_1^2, \ldots, \mathscr{T}_{N_2}^2, \mathscr{T}_0\}$. Then, using Theorem 2, we can find such trajectories as start near $\mathscr{T}_0$, pass near $\mathscr{T}_1^1, \ldots, \mathscr{T}_{N_1}^1$ or near $\mathscr{T}_1^2, \ldots, \mathscr{T}_{N_2}^2$, return near $\mathscr{T}_0$ and repeat these motions eternally. To parts of these trajectories we can assign the symbol '1' or '2', depending on whether they pass near $\mathscr{T}_1^1, \ldots, \mathscr{T}_{N_1}^1$ or near $\mathscr{T}_1^2, \ldots, \mathscr{T}_{N_2}^2$. Hence, there exist *chaotic orbits* characterized by the Bernoulli shift. Thus, in very complicated manners the orbits detected in Theorem 2 can drift near the locally invariant manifolds $\mathscr{M}$.

5. Example

As an example, we consider the Hamiltonian

$$H(x,y) = \frac{1}{2}\left(-x_1^2 + \sum_{l=1}^{n} \omega_l^2 y_l^2\right) + \frac{1}{4}\left(x_1^2 + \sum_{l=1}^{n} \beta_l y_l^2\right)^2 + \frac{1}{2}\left(x_2^2 + \sum_{l=1}^{n} y_{n+l}^2\right) \tag{15}$$

with $l \geq 3$ an integer. When $\beta_l = j_l^2$, the Hamiltonian (15) represents the finite degree-of-freedom model (8) for the buckled beam. Eq. (2) has a pair of homoclinic orbits to the saddle $x = 0$,

$$x_{\pm}^{\mathrm{h}}(t) = (\pm\sqrt{2}\mathrm{sech}t, \mp\sqrt{2}\mathrm{sech}t \tanh t) \tag{16}$$

We assume that the non-resonance condition (3) holds up to fourth-order, so that assumptions (A1)-(A5) hold.

We can compute the Melnikov function

$$M(\theta; r) = \sum_{l=1}^{n} \omega_l^2 r_l^2 b_l \left(a_l \cos(2\theta_l + \phi_l) - b_l\right), \tag{17}$$

where ϕ_l is some constant and

$$a_l = \sqrt{1 + b_l^2}, \quad b_l = \frac{\cos^2(\pi\sqrt{8\beta_l + 1}/2)}{\sinh^2(\pi\omega_l)}.$$

See Section 6 of [15] for the derivation of (17). Using Theorems 1 and 2, we can show that if

$$\beta_l \neq \frac{m(m-1)}{2} \quad m \in \mathbb{N},$$

i.e.,

$$\beta_l \neq 0, 1, 3, 6, 10, 15, \ldots, \tag{18}$$

then for the Hamiltonian (15) transverse homoclinic and heteroclinic orbits to whiskered invariant tori near O exist, and Arnold diffusion type and chaotic motions occur. See [15] for the details. Condition (18) becomes

$$j_l \neq 6, 204, 6930, 235416, \ldots$$

for the bucked beam case. Hence, in the infinite degree-freedom model of buckled beams without the forcing and damping terms, such complicated behavior can occur. See [12] for more details.

6. Numerical evidence of fast diffusion

We now give numerical simulation results for a three-degree-of-freedom system having the Hamiltonian (15) with $n = 2$, $\omega_1 = 1$, $\omega_2 = (\sqrt{5} - 1)/2$ (golden mean), $\beta_1 = 0.5$, $\beta_2 = 1.5$. The code used in the numerical simulations is based on an explicit Runge-Kutta method of order 8 and a fifth order error estimator with third order correction is utilized. It also has a dense output of order 7. See [4] for more details on the method. A tolerance of 10^{-8} was chosen in the computations so that very precise results could be obtained. Actually the changes of the Hamiltonian energy for very long trajectories with $t \sim 10^6$ were 10^{-9} % at most.

We take as a Poincaré section the five-dimensional hyperplane $\{(x, y) \in \mathbb{R}^2 \times \mathbb{R}^4 \mid y_2 = 0, y_4 > 0\}$. To obtain a point at which a computed trajectory intersect the Poincaré section, an interval $[t_{n-1}, t_n]$ of numerical integration such that $y_2(t_{n-1}) < 0$ and $y_2(t_n) \geq 0$ was searched and the method of bisection was used for the interval with a tolerance of $|y_2| < 10^{-8}$.

Figure 4 shows orbits of the Poincaré map restricted on the invariant manifold $\mathcal{M}$, i.e., the y-hyperplane. Only inside the outer circle there can exist orbits with the energy level. As shown in this figure, all computed orbits seemed to construct invariant tori. Note

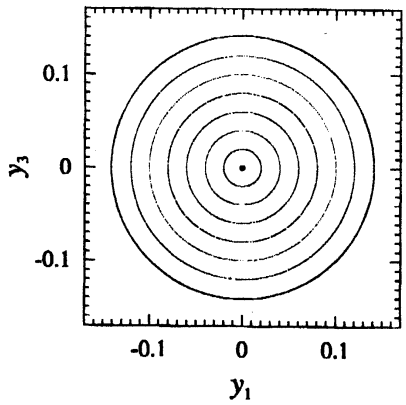

Fig. 4. Numerically computed orbits of the Poincaré map restricted on the invariant manifold $\mathcal{M}$ (the y-hyperplane) for $H = 0.01$.

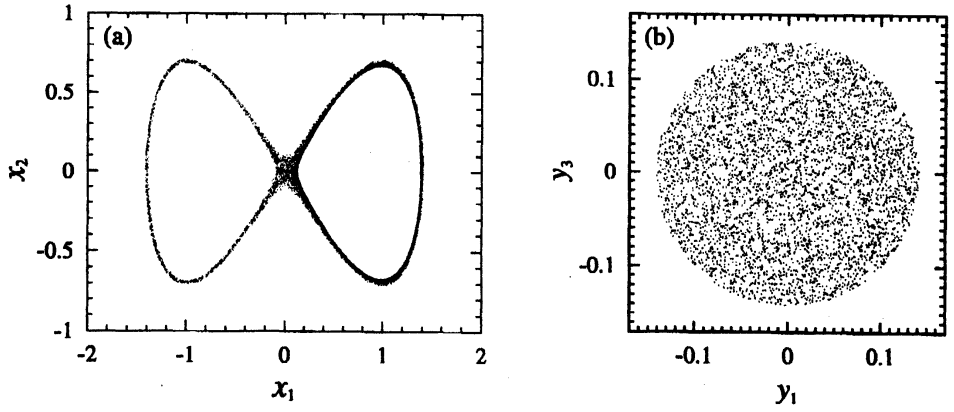

Fig. 5. A numerically computed orbit of the Poincaré map for $\beta_1 = 0.5$, $\beta_2 = 1.5$ and $H = 0.01$: (a) Projection onto the x-plane; (b) projection onto the (y_1, y_3)-plane when it enters in a neighborhood of $\mathcal{M}$.

that orbits of the Poincaré map on $\mathcal{M}$ can move on a two-dimensional manifold by the persistence of the Hamiltonian energy.

Figure 5 shows a numerically computed orbit of the Poincaré map starting at $(x, y) = (0.001, 0.001, 0, 0, 0.099\ldots, 0.1)$. Its projection onto the x-plane is plotted with 20 000 points in Fig. 5(a), and its projection onto the (y_1, y_3)-plane when it enters in a neighborhood of $\mathcal{M}$, $\{(x, y) \,|\, r_x \leq 0.01\}$ with $r_x = \sqrt{x_1^2 + x_2^2}$, is plotted with 5 000 points in Fig. 5(b). From Fig. 5 we see that it does not only exhibit a chaotic motion but also drifts in the center directions of the saddle-center, as stated in Section 5.

Figure 6 shows the second mode energy of the y-component on the Poincaré section (i.e., when $y_2 = 0$), $e_2 = y_4^2/2$, and the distance r_x from the invariant manifold $\mathcal{M}$ for two numerically computed orbits of the Poincaré map with slightly different initial conditions: One of them, which is plotted as dots and solid lines in Fig. 6, started at the same point

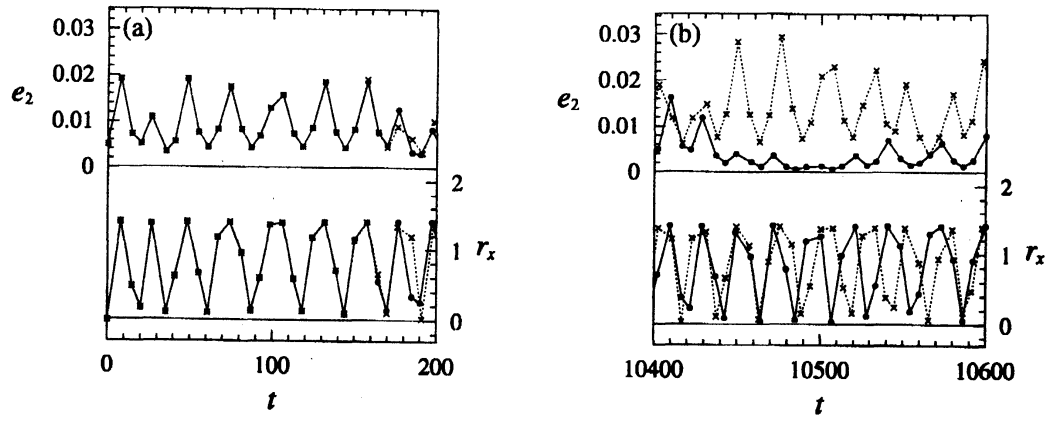

Fig. 6. The second mode energy e_2 of the y-component and the distance r_x from the invariant manifold $\mathcal{M}$ (the y-hyperplane) for two trajectories with slightly different initial conditions for $\beta_1 = 0.5$, $\beta_2 = 1.5$ and $H = 0.01$: (a) small t; (b) large t.

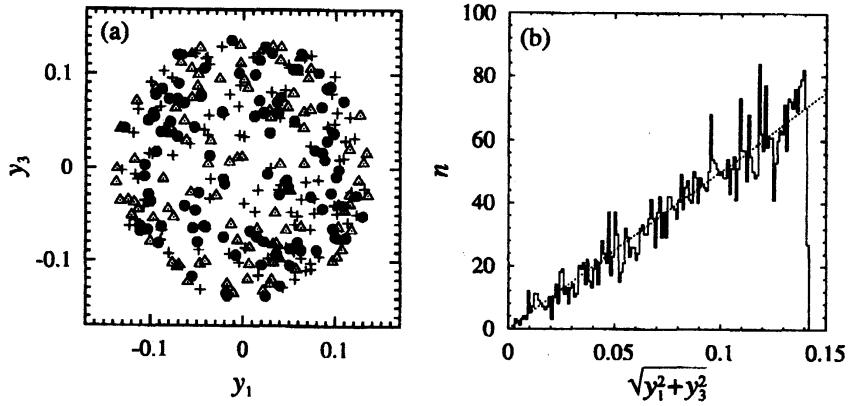

Fig. 7. Homogeneity of motions in the center directions for the orbit of Fig. 5 with $\beta_1 = 0.5$, $\beta_2 = 1.5$ and $H = 0.01$: (a) Projection onto the (y_1, y_3)-plane for first 300 visits in a neighborhood of $\mathcal{M}$; (b) histogram of the density of points with intervals of 1×10^{-3} for the abscissa, $\sqrt{y_1^2 + y_3^2}$, when the orbit enters the neighborhood of $\mathcal{M}$. In Fig. (a) $\times$ represents points for 1st-100th visits, $\bullet$ for 101st-200th, and $\triangle$ for 201st-300th. In Fig. (b) a uniform distribution is also plotted as a broken line for comparison.

as in Fig. 5, and the other, plotted as crosses and broken lines in Fig. 6, started at a point with the same coordinates except $y_1 = 10^{-5}$. We see that both the results are almost the same when t is small (see Fig. 6(a)), but they are very distinct when t is large (see Fig. 6(b)). In particular, the second mode energy e_2 are very different even when the values of r_x are almost simultaneously small at $t \approx 10460$. This means that they are then close to distinct invariant tori far from each other. Thus, their drifts in the center directions sensitively depend on initial conditions and hence they are chaotic, as stated in Section 5.

In Fig. 5(b) one may feel that motions in the center directions are very homogeneous. Figure 7(a) shows projection of the orbit of Fig. 5 onto the (y_1, y_3)-plane for first 300 visits in the neighborhood $\{r_x \leq 0.01\}$ of $\mathcal{M}$, where different symbols are used for every 100 visits (see the caption of Fig. 7), and Figure 7(b) shows a histogram of the density of points of Fig. 5(b) with intervals of 1×10^{-3} for the distance from the origin in the (y_1, y_3)-plane, $\sqrt{y_1^2 + y_3^2}$, where n represents the number of points included in the interval. In Fig. 7(b) a uniform distribution, $c\sqrt{y_1^2 + y_3^2}$, where $c = 2 \times 5000/(2 \times 0.01)$, is also plotted as a broken line for comparison. We see that the orbit visits at very random points in the neighborhood and the distribution of points is close to the uniform one. See [13] for more details.

7. Two-degree-of-freedom systems

In this section, we consider two-dimensional systems of the form

$$\begin{aligned} \dot{x} &= J_1 \mathrm{D}_x H(x, y), \\ \dot{y} &= J_1 \mathrm{D}_y H(x, y), \end{aligned} \qquad (x, y) \in \mathbb{R}^2 \times \mathbb{R}^2 \tag{19}$$

We assume that assumptions (A1)-(A3) and (A5) hold. Note that the non-resonance condition (3) in (A3) has no meaning. Under the assumptions, it follows from the Poincaré center theorem [7] that there exists a one-parameter family of periodic orbits near the origin O. Define the Melnikov function as

$$M(t_0) = q(c_1) - q(B_0 \Phi(\omega t_0) c_1). \tag{20}$$

We can prove that if $M(t_0)$ has a simple zero, then transverse homoclinic orbits to the periodic orbits near O exist. See [11] for the details. Fast diffusion never occurs because each PO has different Hamiltonian energy.

One of recent interesting topics on Hamiltonian systems is the differential Galois theory for their integrability [8]. This theory says that if the normal variational equation along the special solution is nonintegrable as a linear differential equation (roughly speaking, its general solution cannot be represented by elementary functions), then a Hamiltonian system is nonintegrable near a special solution in a meaning of complex functions. We can show that the Galoisian obstructions to integrability along homoclinic orbits and Melnikov criteria for chaos are equivalent. See [14] for the details.

8. Four-dimensional reversible systems

We consider four dimensional systems of the form

$$\dot{x} = f(x, y), \quad \dot{y} = g(x, y), \quad (x, y) \in \mathbb{R}^2 \times \mathbb{R}^2. \tag{21}$$

We make the following assumptions on (21).

(R1) There exists a linear involution $R : \mathbb{R}^2 \times \mathbb{R}^2 \to \mathbb{R}^2 \times \mathbb{R}^2$ such that

$$(f(R(x,y)), g(R(x,y))) + R(f(x,y), g(x,y)) = 0.$$

Moreover, $\dim \mathrm{Fix}(R) = 2$, where $\mathrm{Fix}(R) = \{(x,y) \in \mathbb{R}^4 | R(x,y) = (x,y)\}$.

Assumption (R1) means that the system (21) is *reversible*. A fundamental characteristic of reversible systems is that if $(x(t), y(t))$ is a solution of (21), then $R(x(-t), y(-t))$ is so. We call a solution (and the corresponding orbit) *symmetric* if $x(t) = Rx(-t)$. An orbit is symmetric if and only if it intersects the space $\mathrm{Fix}(R)$.

(R2) The x-plane is invariant, i.e., $g(x,0) = 0$.

(R3) The origin O is a saddle-center and has a homoclinic orbit $(x^{\mathrm{h}}(t), 0)$.

(R4) The restricted system on the x-plain

$$\dot{x} = f(x,0) \tag{22}$$

is Hamiltonian,i.e., $f(x,0) = J_1 \mathrm{D}H(x)$.

It follows from (R1) and (R3) that there exists a one-parameter family of periodic orbits near the saddle-center O [2]. Define the Melnikov function

$$M(t_0) = \int_{-\infty}^{\infty} \mathrm{D}_x H(x^{\mathrm{h}}(t)) \cdot p(x^{\mathrm{h}}(t), \Psi(t) B_-^{-1} \Phi(t_0) e_1) \mathrm{d}t. \tag{23}$$

Suppose that $M(t_0)$ has a simple zero. Then we can prove that there exist transverse homoclinic orbits to the periodic orbits near O. Moreover, as in Theorems 1 and 2, under an additional condition, we can show that there exist transverse heteroclinic orbits to the periodic orbits and fast diffusion occurs. See [16] for the details.

We apply the theory to

$$\begin{aligned} &\dot{x}_1 = x_2, \quad \dot{x}_2 = x_1 - (x_1^2 + \tfrac{1}{2}y_1^2)x_1 - \tfrac{1}{2}\beta y_1^2, \\ &\dot{y}_1 = y_2, \quad \dot{y}_2 = -\omega^2 y_1 - \alpha(x_1^2 + \tfrac{1}{8}y_1^2)y_1 - \beta x_1 y_1, \end{aligned} \tag{24}$$

where α, β and ω are positive constants. Eq. (24) is Hamiltonian when $\alpha = \frac{1}{2}$. We compute the Melnikov function as

$$M(t_0) = I_1 \cos 2\omega t_0 + I_2 \sin 2\omega t_0, \tag{25}$$

where I_1 and I_2 can be numerically estimated.

Figure 8 shows a numerically computed orbit of the Poincaré map for (24) when $\alpha = 1.5$, $\beta = 0.5$ and $\omega = 1$. Here the three dimensional space $\{(x_1, x_2, y_1, y_2) \,|\, y_2 = 0, \dot{y}_2 < 0\}$ was taken as the Poincaré section. We see that diffusion motion occurs in the center direction.

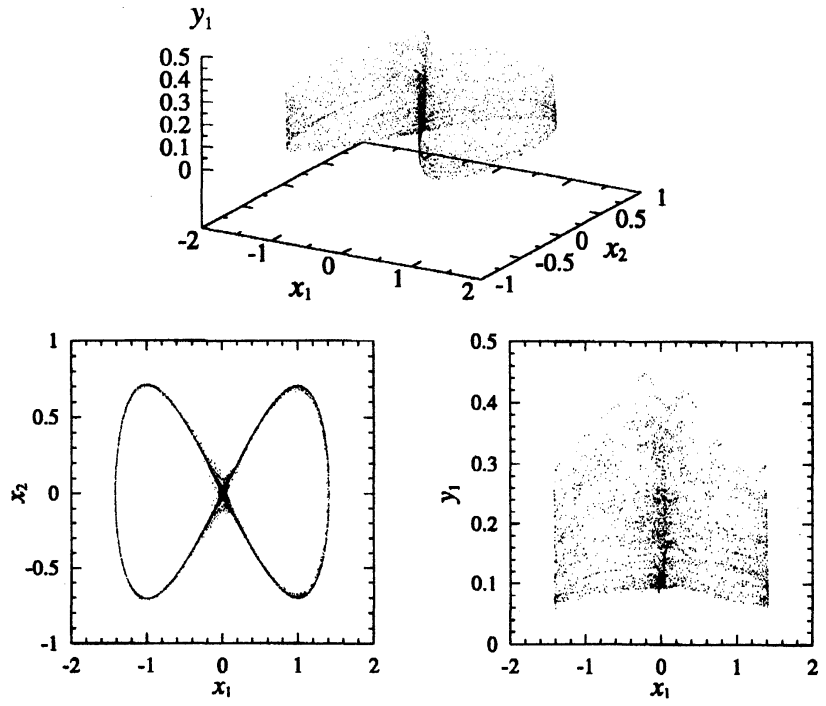

Fig. 8. A numerically computed orbit of the Poincaré map for (24) when $\alpha = 1.5$, $\beta = 0.5$ and $\omega = 1$.

References

[1] E.A. Coddington and N. Levinson, *Theory of Ordinary Differential Equations*, McGraw-Hill, New York, 1955.

[2] R.L. Devaney, Reversible diffeomorphisms and flows, *Trans. Amer. Math. Soc.*, **218** (1976) 89–113.

[3] S.M. Graff, On the conservation of hyperbolic invariant tori for Hamiltonian systems, *J. Diff. Eqns.* **15** (1974), 1–69.

[4] E. Hairer, S.P. Nørsett, G. Wanner, Solving Ordinary Differential Equations I, 2nd ed., Springer, Berlin, 1993.

[5] G. Haller, *Chaos near Resonance*, Springer, New York, 1999.

[6] P.J. Holmes and J.E. Marsden A partial differential equation with infinitely many periodic orbits: chaotic oscillations of a forced beam, *Arch. Rational Mech. Anal.*, **76** (1981), 135–165.

[7] K.R. Meyer and G.R. Hall, *Introduction to Hamiltonian Dynamical Systems and the N-Body Problem*, Springer, New York, 1992.

[8] J.J. Morales-Ruiz, *Differential Galois Theory and Non-Integrability of Hamiltonian systems*, Birkhäuser, Basel, 1999.

[9] A. Vanderbauwhede, Centre manifolds, normal forms and elementary bifurcations in *Dynamics Reported* Vol. 2 (U. Kirchgraber and H. O. Walther, eds.), John Wiley and Sons, Chichester, 1989, pp. 89–169.

[10] S. Wiggins, *Global Bifurcations and Chaos – Analytical Methods*, Springer, New York, 1988.

[11] K. Yagasaki, Horseshoes in two-degree-of-freedom Hamiltonian systems with saddle-centers, *Arch. Rational Mech. Anal.*, **154** (2000), 275–296

[12] K. Yagasaki, Homoclinic and heteroclinic behavior in an infinite-degree-of-freedom Hamiltonian system: Chaotic free vibrations of an undamped, buckled beam *Phys. Lett. A*, **285** (2001), 55–62

[13] K. Yagasaki, Numerical evidence of fast diffusion in a theree-degree-of-freedom Hamiltonian system with a saddle-center, *Phys. Lett. A*, **301** (2002), 45–52.

[14] K. Yagasaki, Galoisian obstructions to integrability and Melnikov criteria for chaos in two-degree-of-freedom Hamiltonian systems with saddle centres *Nonlinearity*, **16** (2003), 2003–2012.

[15] K. Yagasaki, Homoclinic and heteroclinic orbits to invariant tori in multi-degree-of-freedom Hamiltonian systems with saddle-centres. *Nonlinearity*, **18** (2005), 1331–1350.

[16] K. Yagasaki, Homoclinic and heteroclinic orbits to periodic orbits, chaos and diffusion in four-dimensional, non-conservative, reversible systems with saddle-centers, in preparation.